Analog experiments in volcanology: towards multimethod, upscaled and integrated models

Sam Poppe *[1,2], Johan Gilchrist[3,4], Eric Christophe Pascal Breard [4,5], Alison Graettinger[6], Stephen Pansino[7]

1. Centrum Badań Kosmicznych Polskiej Akademii Nauk (CBK PAN), Bartycka 18A, 00-716 Warszawa, Warsaw, Poland
2. Laboratoire G-Time, Department of Geosciences, Environment and Society, Université libre de Bruxelles, Brussels, Belgium
3. Geological Fluid Dynamics Laboratory, Department of Earth, Ocean and Atmospheric Sciences, University of British Columbia, Vancouver, Canada
4. Department of Earth Sciences, University of Oregon, Eugene, OR, USA.
5. School of Geosciences, University of Edinburgh, The King's Building, Edinburgh, Scotland
6. Department of Earth and Environmental Sciences, University of Missouri Kansas City, Kansas City, MO, USA
7. Department of Earth Science, Durham University, Durham, UK

*contact: sampoppe@cbk.waw.pl, sam35poppe@gmail.com

Please refer to this work as:

Poppe, S., Gilchrist, J., Breard, E.C.P., Graettinger, A., Pansino, S. (2022). Analog experiments in volcanology: towards multimethod, upscaled and integrated models. *Bulletin of Volcanology, 84:52.* https://doi.org/10.1007/s00445-022-01543-x

Analog experiments in volcanology: towards multimethod, upscaled and integrated models

Sam Poppe *[1,2], Johan Gilchrist[3,4], Eric Christophe Pascal Breard [4,5], Alison Graettinger[6], Stephen Pansino[7]

1. Centrum Badań Kosmicznych Polskiej Akademii Nauk (CBK PAN), Bartycka 18A, 00-716 Warszawa, Warsaw, Poland
2. Laboratoire G-Time, Department of Geosciences, Environment and Society, Université libre de Bruxelles, Brussels, Belgium
3. Geological Fluid Dynamics Laboratory, Department of Earth, Ocean and Atmospheric Sciences, University of British Columbia, Vancouver, Canada
4. Department of Earth Sciences, University of Oregon, Eugene, OR, USA.
5. School of Geosciences, University of Edinburgh, The King's Building, Edinburgh, Scotland
6. Department of Earth and Environmental Sciences, University of Missouri Kansas City, Kansas City, MO, USA
7. Department of Earth Science, Durham University, Durham, UK

*contact: sampoppe@cbk.waw.pl, sam35poppe@gmail.com

ABSTRACT

For decades scaled analog experiments have improved the understanding of a broad range of multiphase volcanological processes in controlled laboratory environments. Successfully modeled processes include magma flow through magma reservoirs, conduits and sheets, associated crustal deformation, lava flow, volcanic plume dynamics, ash cloud dispersion, pyroclast sedimentation, pyroclastic density currents and debris flows. Prior to the advent of computational modeling in volcanology, analog experiments were the primary method used to test newly developed concepts. Over the past two decades, technological advances have led to increased quantification of model observables, including deformation fields, lava flow rheologies, bubble and particle suspension compositions, runout distances, plume geometries, and rates of ash cloud spreading and sedimentation. For experimental results to yield further insights in volcanic processes and observables directly useful to volcano monitoring efforts, we expect future progress to focus on three major fronts: 1) improved multimethod measurements in experiments; 2) upscaling to near-natural-scale experiments conducted by multidisciplinary teams at internationally shared facilities; and 3) integration with computational models that will guide future geophysical observations and predictions of volcanic activity. This way, analog experiments will bridge gaps between other techniques in volcanology and improve our understanding and forecasting of volcanic activity from the Earth's mantle to the surface and into the atmosphere.

INTRODUCTION

Observing magmatic and volcanic processes is limited to indirect observations of subsurface magma movements using complex geophysical methods, challenging remote sensing techniques, incomplete monitoring networks that produce incompatible data sets, and hazardous field conditions (Loughlin et al. 2015; Fernández et al. 2017). In addition, incomplete preservation and exposure of intrusive, extrusive and pyroclastic deposits permits inferences of dynamic volcanic processes only through a series of assumptions (Alfano et al. 2016; Bertelsen et al. 2021).

Scaled analog experiments overcome some of the above in situ measurement challenges, computer processing power limitations and associated spatial and temporal resolution constraints. Experiments provide insights into dynamic volcanic processes by systematically investigating sets of physical parameters that are critical to interpreting volcano monitoring data and forecasting eruptions and associated hazards (Appendix Table 1; e.g. Leever et al. 2014, Merle 2015, Kavanagh et al. 2018a).

In this contribution, we review the technological progress in the past two decades that has expanded options for quantitative analyses of multidimensional analog experiments modeling volcanic flows and deformation. We then identify three major fronts of progress that will expand the unique role of analog experiments in multidisciplinary volcanological research: improved measurements using multiple methods and instruments (multimethod), upscaling and multimethod integration. Table 1 (Appendix) facilitates directly comparing scaled parameters with volcano monitoring data and testing of conceptual and numerical models. Readers can find more comprehensive reviews of analog experimental studies in volcanology, including magma chamber processes that we omit, in Mader et al. (2004, 2013), Acocella (2007), Galland et al. (2018), Kavanagh et al. (2018a) and Roche and Carazzo (2019), and Rivalta et al. (2015).

ADVANCEMENTS IN ANALOG MODELING IN THE PAST TWO DECADES

Sub-surface magma migration and structural deformation

Magma is channelled from source regions in the Earth's mantle through volcanic and igneous plumbing systems (VIPS) towards eruption at the surface (Burchardt 2018). VIPS were previously seen as melt-dominated simple cylindrical pipes and ball-shaped "chambers". Analog experiments have helped form the current consensual model of intricate networks of geometrically complex reservoirs, conduits and sheets, filled with heterogeneous mixtures of magmatic melt, crystals and exsolved volatiles, that produce seismicity, degassing and ground deformation (Cashman and Sparks 2013; Galland et al. 2018). The use of crustal rock analogs of contrasting rheologies, such as brittle-elastic gelatin vs. plastic granular materials, has underscored the control of magma and host rock properties on the three-dimensional (3D) growth of intrusions and reservoirs and associated deformation (Kavanagh et al. 2018b; Bertelsen et al. 2021). Furthermore, the introduction of faulting, gravitational and far-field forces to analog experiments has helped better understand complex stress interactions between propagating magma, topographic (un)loading and tectonic forces causing acute caldera and flank collapse, or chronic gravitational deformation (e.g. Merle and Borgia 1996; Acocella 2007; Delcamp et al. 2018).

Modern high-speed cameras, photogrammetry, digital image analysis software and even X-ray Computed Tomography and digital volume analysis have driven a methodological evolution from qualitative descriptions to temporal quantitative monitoring of deformation fields in two dimensions (2D) against vertical cross-sections, and in 3D on experiment surfaces (e.g. Acocella 2007; Ruch et al. 2012; Galland et al. 2016) and in the experiment interior (Fig. 1C; Kervyn et al. 2010; Poppe et al. 2019). More realistic physical scaling has been obtained by increasingly detailed analog material characterisation (see Table 1 of Appendix; Kavanagh et al. 2013; Reber et al. 2020; Poppe et al. 2021). Nevertheless, experiments have mostly focused on limited interactions between parameters, and experiments are rarely coupled with numerical methods.

Conduit and surface viscous flow

Shallow conduit flow encompasses a variety of interrelated processes, including volatile exsolution, decompression, multiphase flow dynamics (gas-liquid, solid-fluid, gas-liquid-solid, or two liquids of contrasting viscosity), fragmentation, lava lake dynamics, as well as lava dome extrusions and lava flows (Fig. 1). A focused study of a fundamental process minimizes complexity and dictates experimental design, which branches into three categories: depressurization, magma rheology, volumetric flux and solidification experiments.

Depressurization experiments load rock fragments or viscous liquids into pressurized shock tubes sealed by a releasable diaphragm. The pressure loss allows for modeling of volatile exsolution, bubble growth and fragmentation dynamics (Anilkumar et al. 1993; Spina et al. 2016). Volumetric flux experiments focus on the transport of one or more fluids through a narrow conduit, sometimes with reservoirs fixed to the ends. This allows for the study of one-, two-, and even three-phase flow dynamics, including bidirectional flow and bubble flow regimes (Seyfried and Freundt 2000; Oppenheimer et al. 2020). When a reservoir is fixed to the upper end, surface level fluctuations, funnel geometry and general flow dynamics can act as an analog for lava lakes (Witham et al. 2006; Qin et al. 2018). The physics governing Strombolian eruptions have been modeled in experiments on air bubble rise through relative viscous glucose or syrup, such as the ascent and potential break up of gas slugs, the effect of conduit geometry, the very long period deformation signal, and transitions from churn to annular flow (e.g. Kueppers et al. 2006; Perugini and Kueppers 2012; Pioli et al. 2012; Azzopardi et al. 2014).

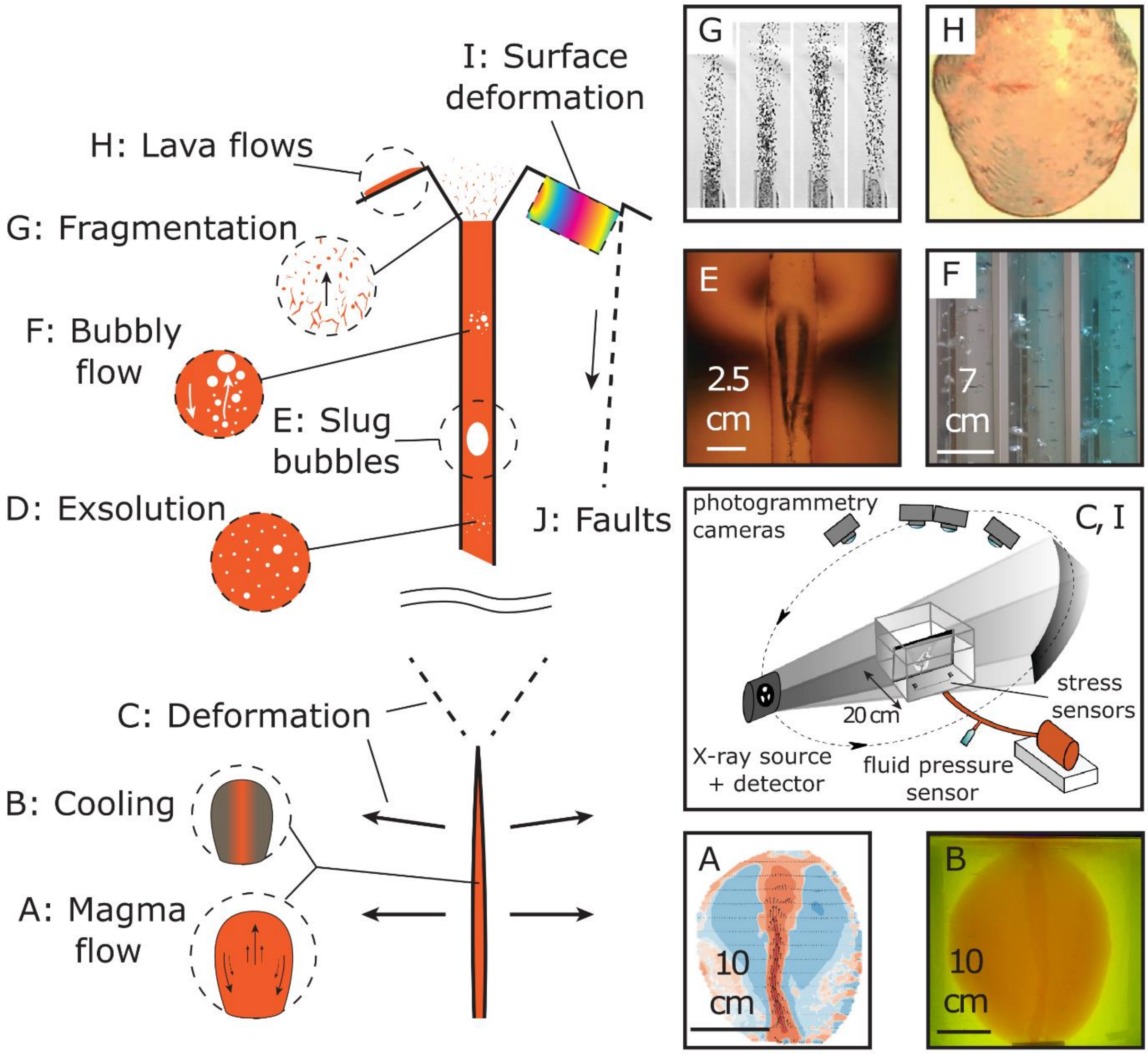

Figure 1. Magma migration takes place primarily through sheet intrusions (depicted below) and conduits (above). Individual processes illustrated in circular insets: (**A**) magma dynamics within a dike, (**B**) dike flow localization, (**C**) host rock deformation, (**D**) volatile exsolution, (**E**) slug ascent, (**F**) bubbly flow, (**G**) fragmentation, (**H**) lava flows, (**I**) (far field) surface deformation, (**J**) fault formation. Photo examples in square insets correspond to: (**A**) Pansino et al. (in prep); (**B**) Pansino et al. (2019a, b); (**C**) Poppe et al. (2019), stress sensors in Seropian and Stix (2018), fluid pressure sensor in Bertelsen et al. (2021); (**E**) Manta et al. (2019); (**F**) Pansino et al. (2019a, b); (**G**) Salvatore et al. (2020) reproduced with permission; (**J**) Dietterich et al. (2017) reproduced with permission.

Finally, solidification experiments omit the conduit and instead model effusive activity, like lava flows, dome extrusion and fragmentation involving external water (e.g. Fink and Griffiths 1990; Cashman et al. 2006; Sonder et al., 2018). Whereas models can use single phase liquid or granular materials to simulate lava flow and dome dynamics (Dietterich et al. 2015; Zorn et al. 2020), solidification experiments rely on materials which cool and undergo heterogeneous solidification (Soule and Cashman 2004), but also have incorporated near-real-scale furnace-heated basalt (e.g. Lev et al. 2012; Edwards et al. 2013; Rumpf et al. 2018). Depending on the source geometry, influx, temperature and substrate roughness, it is thus possible to investigate the velocity and geometry of such features, which strongly resemble natural examples.

Sub-aerial tephra dispersal and ground-hugging flows

Above the surface, the past decade of analog experiments modeling volcanic plumes (Fig. 2a, b), explosive excavation and ballistic ejection (Fig. 2d), debris flows and pyroclastic density currents (PDCs; Fig. 2a, b) have ranged from "small-scale" benchtop flume (e.g., Roche 2012; Sher and Woods 2017; Smith et al. 2020) and tank experiments (Fig. 2b; e.g., Carazzo and Jellinek, 2012; Chojnicki et al. 2015; Gilchrist and Jelinek 2021) to "large-scale" laboratory (e.g., Lube et al. 2015; Breard and Lube 2017; Brosch and Lube 2020), and outdoor experiments (Fig. 2c, d; e.g., Graettinger et al. 2014; Sulpizio et al. 2016; Dellino et al., 2019). These experiments have established new links between micro-scale (particle scale) processes and bulk multiphase flow behavior (Fig. 2a). Two-way particle-fluid coupling processes (e.g., preferential concentration in eddies; Fig. 2a) exert controls on the mass partitioning between collapsing flows, which feed PDCs, or buoyantly rising and spreading flows, which generate plumes and ash clouds (e.g., Jessop and Jellinek 2014; Lherm and Jellinek 2019; Gilchrist and Jellinek 2021). Four-way coupling (e.g., mesoscale clustering) controls the exchange of mass between dilute and dense flow regions in PDCs (e.g., Breard et al. 2016; Brosch and Lube 2020; Weit et al. 2020) and induces triboelectrification in volcanic jets that creates detectable lightning (e.g., Cimarelli et al. 2014; Van Eaton et al. 2016; Méndez Harper et al. 2021). In their densest form, volcanic flows become granular flows dominated by frictional stresses with unexpectedly high mobility and interactions with erodible substrates that can significantly affect their runout (e.g., Iverson et al. 2011; Roche et al. 2013; Bernard et al. 2014). Large-scale experiments show the expulsion of fine particle-gas mixtures from collapsing volcanic flows and have inspired improved numerical simulations and comparison to natural deposits (Graettinger et al. 2014; Valentine 2020). Due to the wide range of particle size distributions in volcanic flows, one-way and two-way particle-fluid coupling can co-exist with four-way coupling in a single system (Fig. 2e, f; e.g., Breard et al. 2016, 2017; Lube et al. 2020).

THREE FRONTS OF PROGRESS

We identify three fronts through which analog experiments can be improved to achieve the ultimate goals of volcano science (Fig. 3): understanding volcanic processes, forecasting volcanic hazards and mitigating these hazards to society.

First, continued progress in *multimethod quantification of model parameters* that govern the dynamics of volcanic flows and deformation will address key knowledge gaps. Currently, distinct subsets of methods have been deployed at separate laboratories. With recent advancements in microcomputer technology and materials science (Zhu et al. 2020), the variety of available instruments, instrument synchronization and choice of analog materials should greatly improve. By equipping experimental setups with multisensor arrays, these improvements should aim to produce quantitative analyses of the combined effects of several modeled parameters simultaneously, including those parameters listed in Table 1 (Appendix). For example, measuring bulk flow scale properties should be combined with measuring strains and stresses of the carrying fluid or host material at the particle scale. Use of materials that achieve mechanical and thermal dynamic similarity with magma and volcanic mixtures will permit experiments to simultaneously investigate poorly understood mechanical and thermal effects (e.g., Moitra et al. 2018; Seropian and Stix 2018; Gilchrist and Jellinek 2021). Inclusive community benchmark exercises should highlight methodological uncertainties and limitations across laboratories, similar to past efforts in tectonic modeling (Klinkmüller et al. 2016). Broadening and diversifying experimental methods, incorporating more multidisciplinary teams, and replacing esoteric jargon with more widely accessible language, will foster a deeper, richer understanding of volcanic processes and encourage experimental innovation, assisted by Table 1 (Appendix).

Second, *upscaling experimental setups* from laboratory scale to near-real scale in dedicated warehouse or outdoor laboratories will facilitate simultaneous measurements of several parameters of volcanic processes that interact over a wide range of scales, by using a diverse and synchronized array of sensors. Building larger experiments requires a large budget and multi-year commitment, that may not be pragmatic for individual research groups.

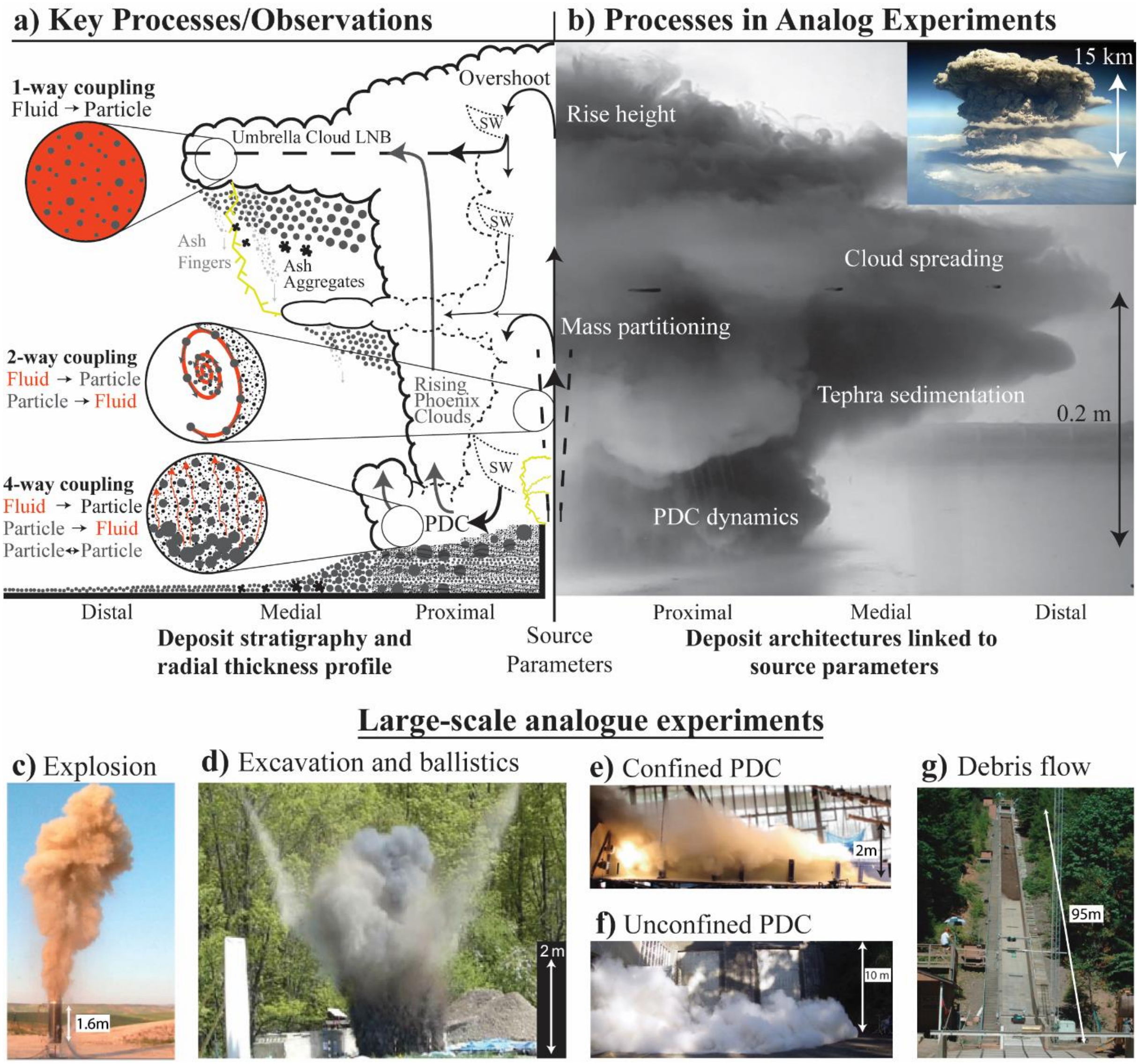

Figure 2: a) Conceptual model of an explosive eruption showing key processes affecting mass transport, hazards and deposition. Exploded circles show particle-scale interactions with fluid phase that affect bulk flow dynamics. **b)** Key investigated processes in a tank-scale experiment modeling Plinian eruptions. **c)** Large-scale outdoor hot ash plume experiment in a quarry, Bari, Italy modeling the fluid mechanics of Vulcanian eruption plumes. Reprinted from Dellino et al. (2010) with permission from John Wiley and Sons. **d)** Large-scale outdoor explosion excavation cratering experiment at the U. Buffalo Geohazards Field Station modeling the mechanics of maar-diatreme eruptions. Reprinted from Graettinger et al. (2014) with permission from John Wiley and Sons. **e-f)** Warehouse and outdoor PDC flow mechanics experiment at the pyroclastic flow eruption large-scale experimental facility (PELE) at Massey U.. Reprinted from Breard et al. (2016) with permission from Springer. **g)** Large-scale outdoor debris flow flume experiments at the U.S. Geological Survey's H. J. Andrews Experimental Forest in Blue River, OR testing suites of monitoring instruments. Reprinted from Iverson et al. (2010) with permission from John Wiley and Sons.

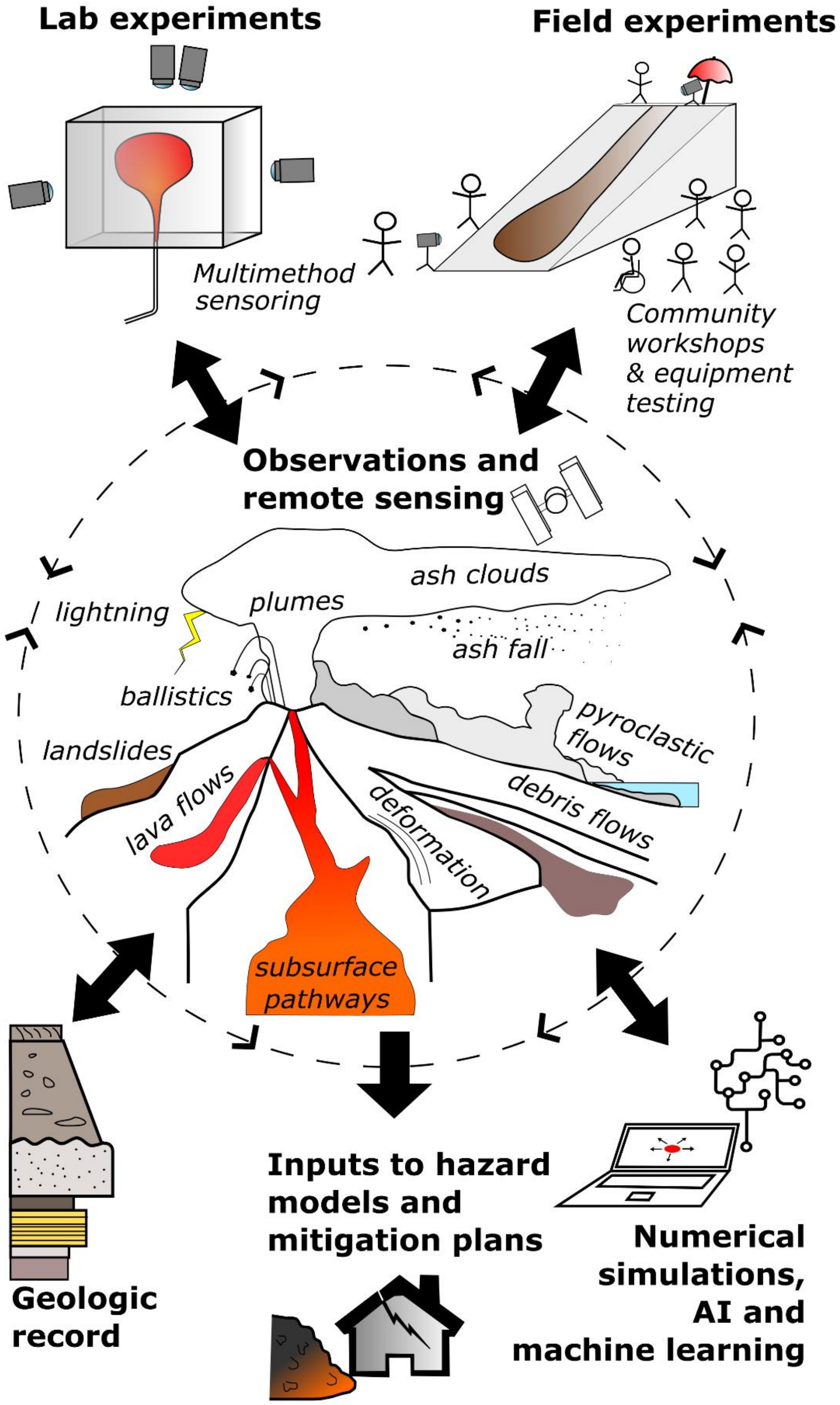

Figure 3. Visual representation of the many ways that analog experiments across a range of scales should integrate with other techniques in volcano science. Experiments are inspired by observations of natural phenomena, used to test and inform the interpretation of the geologic record, and can be coupled with numerical models to improve volcanic hazard models and crisis mitigation plans. Experiments should also be used to test equipment and techniques for future use during eruptions, facilitate discussions at community workshops and engage the wider public.

Multisensor arrays should be deployed during future large-scale explosion, lava flow, column collapse and PDC, lahar and debris flow experiments during community workshops or consortium projects supported by national and international funding bodies at existing large-scale experimental facilities (Iverson et al. 2010; Graettinger et al. 2014; Taddeucci et al. 2015; Breard et al. 2016; Allstadt et al. 2020). The resulting synchronized multiparameter datasets can be used to:

1) Compare to existing multiparameter eruption datasets to better constrain governing volcanic flow parameters;

2) Inform volcano monitoring network design, so that new multisensor arrays are set up to acquire the maximum amount of information for the allotted budget.

The opportunity of inviting the public to attend experiments at outdoor facilities or broadly distribute experiment media on social media and to schools should be exploited more to increase public awareness of volcanic processes.

Third, progress in understanding volcanic processes will come from an *increased integration of laboratory experiments with numerical models*. Whereas experiments have demonstrated capability to model fundamental volcanic processes, knowledge gaps remain due to issues of scale or complexity. The first and second fronts will resolve scaling and upscaling, expose experimental limitations and increase compatibility of experimental data sets with geophysical monitoring data from active volcanoes. Complexity instead calls for careful planning to ensure that each component (e.g., geometry, flow dynamics, and thermodynamics of each material) is properly scaled. Analog experiments are rarely used to guide, calibrate and validate analytical and numerical models, but have shown tremendous capability in this regard (e.g., Maccaferri et al. 2019; Esposti Ongaro et al. 2020; Mantiloni et al., 2021). Extensive and multiparameter experimental data sets can be produced that avoid the limitations of in-situ volcano monitoring data, such as a scarcity of natural events, poorly constrained source and boundary conditions, logistical and technological challenges, or slow processes that occur over a long time frame. Such synthetic data sets will support further testing and development of existing and newly-developed numerical methods, data assimilation, machine learning and artificial intelligence (AI) algorithms (e.g., Albino et al. 2020; Valentine 2020; Watson 2020).

In conclusion, small- to large-scale analog experiments continue to advance into sophisticated, multimethod approaches with increased measurement precision and scaling accuracy for characterizing complex multiphase volcanic processes in space and time. The three identified fronts of progress will help analog experiments continue to improve:

1) Multimethod quantification of multiphase processes;

2) Testing of multisensor volcano monitoring arrays by upscaling experiments to near-natural scales;

3) Increased integration of laboratory experiments with numerical models, machine learning and other AI algorithms.

These efforts will require the mobilization of an increasingly diverse and multidisciplinary community of researchers spanning all career stages, ethnic and national backgrounds in community-wide workshops and consortia supported by scientific associations and funding bodies. In this way, we foresee analog experiments as continuing to contribute uniquely to advances in our ability to model, understand and forecast volcanic hazards and to create opportunities to engage the public over the coming decade.

Acknowledgments This work results from an inspiring exchange between SPo and JGi after AGU 2020 session V018. The helpful comments of G. Valentine, an anonymous reviewer and editors K. Cashman and A. Harris have greatly improved this manuscript.

Author contribution SPo led the writing; all the authors contributed equally. SPa produced Fig. 1, JGi produced Fig. 2, AGr and SPo produced Fig. 3, JGi produced Table 1 (Appendix) with input from all authors. All authors read and approved the final manuscript.

Funding SPo was supported through a frs-F.N.R.S. postdoctoral grant at UIB, and now at SRC PAS by a ULAM scholarship (Polish National Agency for Academic Exchange) and Norway Financial Mechanism grant 2020/37/K/ST10/02447 (NCN Poland). JTG was supported through an NSERC Discovery grant to AM Jellinek. ECBP was supported by NSF grant 1852569 (PI: Joe Dufek). SPa was supported by a Royal Society – Newton International Fellowship, number NIF\R1\202137.

REFERENCES

Abdelmalak MM, Bulois C, Mourgues R, et al (2016) Description of new dry granular materials of variable cohesion and friction coefficient: Implications for laboratory modeling of the brittle crust. Tectonophysics 684:39–51. https://doi.org/10.1016/j.tecto.2016.03.003

Acocella V (2007) Understanding caldera structure and development: An overview of analogue models compared to natural calderas. Earth-Science Rev 85:125–160. https://doi.org/10.1016/j.earscirev.2007.08.004

Albino F, Biggs J, Yu C, Li Z (2020) Automated Methods for Detecting Volcanic Deformation Using Sentinel-1 InSAR Time Series Illustrated by the 2017–2018 Unrest at Agung, Indonesia. J Geophys Res Solid Earth 125:1–40. https://doi.org/10.1029/2019JB017908

Alfano F, Bonadonna C, Watt S, et al (2016) Reconstruction of total grain size distribution of the climactic phase of a long-lasting eruption: the example of the 2008–2013 Chaitén eruption. Bull Volcanol 78:. https://doi.org/10.1007/s00445-016-1040-5

Allstadt KE, Farin M, Iverson RM, et al (2020) Measuring Basal Force Fluctuations of Debris Flows Using Seismic Recordings and Empirical Green's Functions. J Geophys Res Earth Surf 125:. https://doi.org/10.1029/2020JF005590

Andrews BJ, Manga M (2012) Experimental study of turbulence, sedimentation, and coignimbrite mass partitioning in dilute pyroclastic density currents. J Volcanol Geotherm Res 225:30-44 https://doi.org/10.1016/j.jvolgeores.2012.02.011

Anilkumar AV, Sparks RSJ, Sturtevant B (1993) Geological implications and applications of high-velocity two-phase flow experiments. J Volcanol Geotherm Res 56:145–160. https://doi.org/https://doi.org/10.1016/0377-0273(93)90056-W

Azzopardi BJ, Pioli L, Abdulkareem LA (2014) The properties of large bubbles rising in very viscous liquids in vertical columns. Int J Multiph Flow 67:160-173. https://doi.org/10.1016/j.ijmultiphaseflow.2014.08.013

Bernard J, Kelfoun K, Le Pennec J-L, Vallejo Vargas S (2014) Pyroclastic flow erosion and bulking processes; comparing field-based vs. modeling results at Tungurahua Volcano, Ecuador. Bull Volcanol 76(9):1-16, doi:http://dx.doi.org/10.1007/s00445-014-0858-y

Bertelsen HS, Guldstrand F, Sigmundsson F, et al (2021) Beyond elasticity: Are Coulomb properties of the Earth's crust important for volcano geodesy? J Volcanol Geotherm Res 410:. https://doi.org/10.1016/j.jvolgeores.2020.107153

Breard ECP, Lube G (2017) Inside pyroclastic density currents – uncovering the enigmatic flow structure and transport behaviour in large-scale experiments. Earth Planet Sci Lett 458:22-36. doi:http://dx.doi.org/10.1016/j.epsl.2016.10.016.

Breard ECP, Lube G, Jones JR, et al (2016) Coupling of turbulent and non-turbulent flow regimes within pyroclastic density currents. Nat Geosci 9:767–771. https://doi.org/10.1038/ngeo2794

Breard ECP, Dufek J, Lube G (2017) Enhanced Mobility in Concentrated Pyroclastic Density Currents: An Examination of a Self-Fluidization Mechanism. Geophys R Lett 45:654–664. doi:10.1002/2017GL075759.

Breard EC, Jones JR, Fullard L, et al (2019) The permeability of volcanic mixtures—implications for pyroclastic currents. J Geophys Res Solid Earth 124(2):1343-60 https://doi.org/10.1029/2018JB016544

Breard EC, Dufek J, Fullard L, Carrara A (2020) The Basal Friction Coefficient of Granular Flows With and Without Excess Pore Pressure: Implications for Pyroclastic Density Currents, Water-Rich Debris Flows, and Rock and Submarine Avalanches. J Geophys Res Solid Earth 125(12):e2020JB020203 https://doi.org/10.1029/2020JB020203

Brosch E, Lube G (2020) Spatiotemporal sediment transport and deposition processes in experimental dilute pyroclastic density currents. J Volc Geotherm Res 401:106946 https://doi.org/10.1016/j.jvolgeores.2020.106946

Brothelande E, Peltier A, Got JL, et al (2016) Constraints on the source of resurgent doming inferred from analogue and numerical modeling — Implications on the current feeding system of the Yenkahe dome–Yasur volcano complex (Vanuatu). J Volcanol Geotherm Res 322:225–240. https://doi.org/10.1016/j.jvolgeores.2015.11.023

Burchardt S (2018) Introduction to Volcanic and Igneous Plumbing Systems—Developing a Discipline and Common Concepts. In: Burchardt S (ed) Volcanic and Igneous Plumbing Systems. Elsevier, Amsterdam, pp 1–12

Byrne PK, Holohan EP, Kervyn M, et al (2013) A sagging-spreading continuum of large volcano structure. Geology 41:339–342. https://doi.org/10.1130/G33990.1

Cagnoli B, Manga M (2003) Pumice-pumice collisions and the effect of the impact angle. Geophys Res Lett 30(12) https://doi.org/10.1029/2003GL017421

Carazzo G, Jellinek AM (2012) A new view of the dynamics, stability and longevity of volcanic clouds. Earth Planet

Sci Lett 325:39–51. https://doi.org/https://doi.org/10.1016/j.epsl.2012.01.025
Carazzo G, Girault F, Aubry T, et al (2014) Laboratory experiments of forced plumes in a density-stratified crossflow and implications for volcanic plumes. Geophys Res Lett 41(24):8759-66 https://doi.org/10.1002/2014GL061887
Carazzo G, Kaminski E, Tait S (2015) The timing and intensity of column collapse during explosive volcanic eruptions. Earth Planet Scie Lett 411:208-17 https://doi.org/10.1016/j.epsl.2014.12.006
Carey SN, Sigurdsson H, Sparks RS (1988) Experimental studies of particle-laden plumes. J Geophys Res Solid Earth 93(B12):15314-28 https://doi.org/10.1029/JB093iB12p15314
Cashman KV, Stephen R, Sparks J (2013) How volcanoes work: A 25 year perspective. Bull Geol Soc Am 125:664–690. https://doi.org/10.1130/B30720.1
Cashman KV, Kerr RC, Griffiths RW (2006) A laboratory model of surface crust formation and disruption on lava flows through non-uniform channels. Bull Volcanol 68:753–770. https://doi.org/10.1007/s00445-005-0048-z
Chojnicki KN, Clarke AB, Phillips JC, Adrian RJ (2015). Rise dynamics of unsteady laboratory jets with implications for volcanic plumes. Earth Planet Scie Lett 412:186–196. https://doi.org/10.1016/j.epsl.2014.11.046
Cimarelli C, Alatorre-Ibargüengoitia MA, Kueppers U, et al (2014) Experimental generation of volcanic lightning. Geology 42:79–82. https://doi.org/10.1130/G34802.1
Delcamp A, van Wyk de Vries B, James MR (2008) The influence of edifice slope and substrata on volcano spreading. J Volcanol Geotherm Res 177:925–943. https://doi.org/10.1016/j.jvolgeores.2008.07.014
Delcamp A, Poppe S, Detienne M, Paguican EMR (2018) Destroying a Volcanic Edifice—Interactions Between Edifice Instabilities and the Volcanic Plumbing System. In: Volcanic and Igneous Plumbing Systems. Elsevier, pp 231–257
Dellino P, Büttner R, Dioguardi F, et al (2010) Experimental evidence links volcanic particle characteristics to pyroclastic flow hazard. Earth Planet Scie Lett 295(1-2):314-20 https://doi.org/10.1016/j.epsl.2010.04.022
Dellino P, Dioguardi F, Doronzo DM, Mele D (2019) The Entrainment Rate of Non-Boussinesq Hazardous Geophysical Gas-Particle Flows: An Experimental Model With Application to Pyroclastic Density Currents. Geophys Res Lett 46:12851–12861. https://doi.org/10.1029/2019GL084776
Dellino P, Mele D, Bonasia R, et al (2005) The analysis of the influence of pumice shape on its terminal velocity. Geophys Res Lett 32(21) https://doi.org/10.1029/2005GL023954
Dellino P, Zimanowski B, Büttner R, et al (2007) Large-scale experiments on the mechanics of pyroclastic flows: Design, engineering, and first results. J Geophys Res Solid Earth 112(B4) https://doi.org/10.1029/2006JB004313
Derrien A, Taisne B (2019) 360 intrusions in a miniature volcano: Birth, growth, and evolution of an analog edifice. Front Earth Sci 7:. https://doi.org/10.3389/feart.2019.00019
Dietterich HR, Cashman KV, Rust AC, Lev E (2015) Diverting lava flows in the lab. Nature geoscience 8(7):494-496. https://doi.org/10.1038/ngeo2470
Dietterich HR, Lev E, Chen J, et al (2017) Benchmarking computational fluid dynamics models of lava flow simulation for hazard assessment, forecasting, and risk management. J Appl Volcanol 6:. https://doi.org/10.1186/s13617-017-0061-x
Druitt TH, Avard G, Bruni G, et al (2007) Gas retention in fine-grained pyroclastic flow materials at high temperatures. Bull Volcanol 69(8):881-901 https://doi.org/10.1007/s00445-007-0116-7
Dufek J, Wexler J, Manga M (2009) Transport capacity of pyroclastic density currents: Experiments and models of substrate-flow interaction. J Geophys Res Solid Earth 114(B11) https://doi.org/10.1029/2008JB006216
Dürig T, Gudmundsson MT, Dellino P (2015) Reconstruction of the geometry of volcanic vents by trajectory tracking of fast ejecta-the case of the Eyjafjallajökull 2010 eruption (Iceland). Earth Planets Space 67(1):1-8 https://doi.org/10.1186/s40623-015-0243-x
Edwards BR, Karson J, Wysocki R, et al (2013) Insights on lava–ice/snow interactions from large-scale basaltic melt experiments. Geology 41(8):851-4. https://doi.org/10.1130/G34305.1
Esposti Ongaro T, Cerminara M, Charbonnier SJ, et al (2020) A framework for validation and benchmarking of pyroclastic current models. Bull Volcanol 82(6):51. https://doi:10.1007/s00445-020-01388-2.
Fauria KE, Manga M (2018) Pyroclast cooling and saturation in water. J Volcanol Geotherm Res 362:17-31 https://doi.org/10.1016/j.jvolgeores.2018.07.002
Fernández J, Pepe A, Poland MP, Sigmundsson F (2017) Volcano Geodesy: Recent developments and future challenges. J Volcanol Geotherm Res 344:1–12. https://doi.org/10.1016/j.jvolgeores.2017.08.006
Fink JH, Griffiths RW (1990) Radial spreading of viscous-gravity currents with solidifying crust. J Fluid Mech 221:485–509. https://doi.org/10.1017/S0022112090003640
Gailler L-S, Lénat J-F, Lambert M, et al (2009) Gravity structure of Piton de la Fournaise volcano and inferred mass

transfer during the 2007 crisis. J Volcanol Geotherm Res 184:31–48. https://doi.org/10.1016/j.jvolgeores.2009.01.024
Galland O, Cobbold PR, Hallot E, et al (2006) Use of vegetable oil and silica powder for scale modelling of magmatic intrusion in a deforming brittle crust. Earth Planet Sci Lett 243:786–804. https://doi.org/10.1016/j.epsl.2006.01.014
Galland O, Burchardt S, Hallot E, et al (2014) Toward a unified dynamic model for dykes and cone sheets in volcanic systems. 16:5468
Galland O, Bertelsen HS, Guldstrand F, et al (2016) Application of open-source photogrammetric software MicMac for monitoring surface deformation in laboratory models. J Geophys Res Earth 1–21. https://doi.org/10.1002/2015JB012755.Received
Galland O, Holohan EP, van Wyk de Vries B, Burchardt S (2018) Laboratory Modelling of Volcano Plumbing Systems: A Review. In: Breitkreuz C, Rocchi S (eds) Physical Geology of Shallow Magmatic Systems - Dykes, Sills and Laccoliths. Springer Berlin Heidelberg, pp 147–214
Gilchrist JT, Jellinek AM (2021) Sediment waves and the gravitational stability of volcanic jets. Bull Volcanol 83:. https://doi.org/10.1007/s00445-021-01472-1
Gilchrist J, Mergny C, Rowell CR, et al (2020) Characterization of source unsteadiness and entrainment into explosive eruptions using laboratory-and field-based methods. AGU Fall Meeting Abstracts 2020:V008-0014. https://ui.adsabs.harvard.edu/abs/2020AGUFMV008.0014G
Gonnermann HM (2015) Magma fragmentation. Annu Rev Earth Planet Sci 43:431–458. https://doi.org/10.1146/annurev-earth-060614-105206
Gonnermann HM, Giachetti T, Fliedner C, et al (2017) Permeability during magma expansion and compaction. J Geophys Res Solid Earth 122(12):9825-48 https://doi.org/10.1002/2017JB014783
Graettinger AH (2018) Trends in maar crater size and shape using the global Maar Volcano Location and Shape (MaarVLS) database. J Volcanol Geotherm Res 357:1-3. https://doi.org/10.1016/j.jvolgeores.2018.04.002
Graettinger AH, Valentine GA (2017) Evidence for the relative depths and energies of phreatomagmatic explosions recorded in tephra rings. Bull Volcanol 79(12):1-21. https://doi.org/10.1007/s00445-017-1177-x
Graettinger AH, Valentine GA, Sonder I, et al (2014) Maar-diatreme geometry and deposits: Subsurface blast experiments with variable explosion depth. Geochemistry, Geophys Geosystems 15:740–764. https://doi.org/10.1002/2013GC005198
Gregg TK, Fink JH (2000) A laboratory investigation into the effects of slope on lava flow morphology. J Volcanol Geotherm Res 96(3-4):145-59 https://doi.org/10.1016/S0377-0273(99)00148-1
Griffiths RW (2000) The dynamics of lava flows. Ann Rev Fluid Mech 32(1):477-518. https://doi.org/10.1146/annurev.fluid.32.1.477
Grosse P, Poppe S, Delcamp A, et al (2020) Volcano growth versus deformation by strike-slip faults: Morphometric characterization through analogue modelling. Tectonophysics. https://doi.org/10.1016/j.tecto.2020.228411
Guldstrand, F., Burchardt, S., Hallot, E., Galland, O. (2017) Dynamics of surface deformation induced by dikes and cone sheets in a cohesive Coulomb brittle crust. J Geophys Res Solid Earth 122(10):8511-8524. https://doi.org/10.1002/2017JB014346
Hartlieb P, Toifl M, Kuchar F, et al (2016) Thermo-physical properties of selected hard rocks and their relation to microwave-assisted comminution. Miner Eng 91:34–41. https://doi.org/10.1016/j.mineng.2015.11.008
Holohan EP, Van Wyk de Vries B, Troll VR (2008) Analogue models of caldera collapse in strike-slip tectonic regimes. Bull Volcanol 70:773–796. https://doi.org/10.1007/s00445-007-0166-x
Huppert HE (1982) The propagation of two-dimensional and axisymmetric viscous gravity currents over a rigid horizontal surface. J Fluid Mech 121:43-58. https://doi:10.1017/S0022112082001797
Huppert HE, Sparks, RSJ (1985) Cooling and contamination of mafic and ultramafic magmas during ascent through continental crust. Earth Planet Scie Lett 74(4):371-386. https//doi.org/10.1016/S0012-821X(85)80009-1
Huppert HE, Sparks RSJ, Turner JS, Arndt NT (1984) Emplacement and cooling of komatiite lavas. Nature 309(5963):19-22. https://doi.org/10.1038/309019a0
Iverson RM (2012) Elementary theory of bed-sediment entrainment by debris flows and avalanches. J Geophys Res Earth Surf 117(F3). https://doi.org/10.1029/2011JF002189
Iverson RM, Logan M, LaHusen RG, Berti M (2010) The perfect debris flow? Aggregated results from 28 large-scale experiments. J Geophys Res 115:. https://doi.org/10.1029/2009jf001514
Iverson RM, Reid ME, Logan M, et al (2011) Positive feedback and momentum growth during debris-flow entrainment of wet bed sediment. Nat Geosci 4:116–121. https://doi.org/10.1038/ngeo1040
Jessop D, Jellinek A (2014) Effects of particle mixtures and nozzle geometry on entrainment into volcanic jets.

Geophys Res Lett 41(11):3858–3863. https://doi.org/10.1002/2014GL060059
Jessop DE, Gilchrist J, Jellinek AM, Roche O (2016) Are eruptions from linear fissures and caldera ring dykes more likely to produce pyroclastic flows? Earth Planet Scie Lett 454:142-53. https://doi.org/10.1016/j.epsl.2016.09.005
Kavanagh JL, Menand T, Daniels KA (2013) Gelatine as a crustal analogue: Determining elastic properties for modelling magmatic intrusions. Tectonophysics 582:101–111. https://doi.org/10.1016/j.tecto.2012.09.032
Kavanagh JL, Engwell S, Martin S (2018a) A review of analogue and numerical modelling in volcanology. Solid Earth 9:531–571. https://doi.org/10.5194/se-9-531-2018
Kavanagh JL, Burns AJ, Hilmi Hazim S, et al (2018b) Challenging dyke ascent models using novel laboratory experiments: Implications for reinterpreting evidence of magma ascent and volcanism. J Volcanol Geotherm Res 354:87–101. https://doi.org/10.1016/j.jvolgeores.2018.01.002
Kervyn M, Boone MN, de Vries B van W, et al (2010) 3D imaging of volcano gravitational deformation by computerized X-ray micro-tomography. Geosphere 6:482–498. https://doi.org/10.1130/ges00564.1
Kieffer SW, Sturtevant B (1984) Laboratory studies of volcanic jets. J Geophys Res Solid Earth 89(B10):8253-68. https://doi.org/10.1029/JB089iB10p08253
Kilgour G, Manville V, Della Pasqua F, et al (2010) The 25 September 2007 eruption of Mount Ruapehu, New Zealand: directed ballistics, surtseyan jets, and ice-slurry lahars. J Volcanol Geotherm Res 191(1-2):1-4. https://doi.org/10.1016/j.jvolgeores.2009.10.015
Klinkmüller M, Schreurs G, Rosenau M, Kemnitz H (2016) Properties of granular analogue model materials: A community wide survey. Tectonophysics 684:23–38. https://doi.org/10.1016/j.tecto.2016.01.017
Kueppers U, Scheu B, Spieler O, Dingwell DB (2006) Fragmentation efficiency of explosive volcanic eruptions: A study of experimentally generated pyroclasts. J Volcanol Geotherm Res 153(1-2):125-135. https://doi.org/10.1016/j.jvolgeores.2005.08.006
Leever K, Galland O, Acocella V (2014) The science behind laboratory-scale models of the earth. Eos (Washington DC) 95:30. https://doi.org/10.1002/2014EO030008
Lev E, Spiegelman M, Wysocki RJ, Karson JA (2012) Investigating lava flow rheology using video analysis and numerical flow models. J Volcanol Geotherm Res 247:62-73. https://doi.org/10.1016/j.jvolgeores.2012.08.002
Lherm V, Jellinek AM (2019) Experimental constraints on the distinct effects of ash, lapilli, and larger pyroclasts on entrainment and mixing in volcanic plumes. Bull Volcanol 81(12):73. https://doi:10.1007/s00445-019-1329-2.
Lister J, Kerr R (1991) Fluid-Mechanical Models of Crack Propagation and Their Application to Magma Transport in Dykes. J Geophys Res 96:10,049-10,077. https://doi.org/10.1029/91JB00600
Loughlin SC, Sparks S, Brown SK, et al (2015) Global volcanic hazards and risk. Cambridge University Press, Cambridge
Lube G, Breard EC, Cronin SJ et al (2014) Dynamics of surges generated by hydrothermal blasts during the 6 August 2012 Te Maari eruption, Mt. Tongariro, New Zealand. J Volcanol Geotherm Res 286:348–366. https:// doi. org/ 10. 1016/j. jvolg eores. 2014. 05. 010
Lube G, Breard ECP, Cronin SJ, Jones J (2015) Synthesizing large-scale pyroclastic flows: Experimental design, scaling, and first results from PELE. J Geophys Res Solid Earth 120:1487–1502. https://doi.org/10.1002/2014JB011666
Lube G, Breard ECP, Esposti-Ongaro T, et al (2020) Multiphase flow behaviour and hazard prediction of pyroclastic density currents. Nat Rev Earth Environ 1:348–365. https://doi.org/10.1038/s43017-020-0064-8
Maccaferri F, Smittarello D, Pinel V, Cayol V (2019) On the Propagation Path of Magma-Filled Dikes and Hydrofractures: The Competition Between External Stress, Internal Pressure, and Crack Length. Geochemistry, Geophys Geosystems 20:2064–2081. https://doi.org/10.1029/2018GC007915
Mader HM, Manga M, Koyaguchi T (2004) The role of laboratory experiments in volcanology. J Volcanol Geotherm Res 129:1–5. https://doi.org/10.1016/S0377-0273(03)00228-2
Mader HM, Llewellin EW, Mueller SP (2013) The rheology of two-phase magmas: A review and analysis. J Volcanol Geotherm Res 257:135–158. https://doi.org/10.1016/J.JVOLGEORES.2013.02.014
Manta F, Emadzadeh A, Taisne B (2019) New Insight Into a Volcanic System: Analogue Investigation of Bubble-Driven Deformation in an Elastic Conduit. J Geophys Res Solid Earth 124:11274–11289. https://doi.org/10.1029/2019JB017665
Mantiloni L, Davis T, Gaete Rojas AB, Rivalta E (2021) Stress Inversion in a Gelatin Box: Testing Eruptive Vent Location Forecasts With Analog Models. Geophys Res Lett 48:1–11. https://doi.org/10.1029/2020GL090407

Mathieu L, van Wyk de Vries B, Holohan EP, Troll VR (2008) Dykes, cups, saucers and sills: Analogue experiments on magma intrusion into brittle rocks. Earth Planet Sci Lett 271:1–13. https://doi.org/10.1016/j.epsl.2008.02.020

Méndez Harper J, Cimarelli C, Cigala V, et al (2021) Charge injection into the atmosphere by explosive volcanic eruptions through triboelectrification and fragmentation charging Earth Planet Sci Lett 574:117162. https://doi.org/10.1016/j.epsl.2021.117162.

Meredith PG, Atkinson BK (1985) Fracture toughness and subcritical crack growth during high-temperature tensile deformation of Westerly granite and Black gabbro. Phys Earth Planet Inter 39:33–51. https://doi.org/10.1016/0031-9201(85)90113-X

Merle O (2015) The scaling of experiments on volcanic systems. Front Earth Sci 3:1–15. https://doi.org/10.3389/feart.2015.00026

Merle O, Borgia A (1996) Scaled experiments of volcanic spreading. J Geophys Res 101:13805. https://doi.org/10.1029/95JB03736

Moitra P, Sonder I, Valentine GA (2018) Effects of Size and Temperature-Dependent Thermal Conductivity on the Cooling of Pyroclasts in Air. Geochem Geophys Geosystems 19(10):3623-3636. https://doi.org/10.1029/2018GC007510.

Neilsen TB, Matoza RS, Maher S, et al (2019) Preliminary analyses of seismo-acoustic wave propagation in outdoor field-scale analog volcanic explosions. J Acoustic Soc Am 145(3):1869. https://doi.org/10.1121/1.5101754

Oppenheimer J, Rust AC, Cashman KV, Sandnes B (2015) Gas migration regimes and outgassing in particle-rich suspensions. Frontiers Phys 3:60. https://doi.org/10.3389/fphy.2015.00060

Oppenheimer J, Capponi A, Cashman K V, et al (2020) Analogue experiments on the rise of large bubbles through a solids-rich suspension: A “weak plug” model for Strombolian eruptions. Earth Planet Sci Lett 531:115931. https://doi.org/10.1016/J.EPSL.2019.115931

Orescanin MM, Prisco D, Austin JM, Kieffer SW (2014) Flow of supersonic jets across flat plates: Implications for ground-level flow from volcanic blasts. J Geophys Res Solid Earth 119(4):2976-87. https://doi.org/10.1002/2013JB010743

Ort MH, Lefebvre NS, Neal CA, et al (2018) Linking the Ukinrek 1977 maar-eruption observations to the tephra deposits: new insights into maar depositional processes. J Volcanol Geotherm Res 360:36-60. https://doi 10.1016/j.jvolgeores.2018.07.005.

Pansino S, Taisne B (2019) How magmatic storage regions attract and repel propagating dikes. J Geophys Res Solid Earth 124(1):274-90. https://doi.org/10.1029/2018JB016311

Pansino S, Calder ES, Menand T (2019a) Experimental analysis of bubble-driven magma motion in the conduit, for persistently active, open-vent volcanoes. Bull Volcanol 81:. https://doi.org/10.1007/s00445-019-1339-0

Pansino S, Emadzadeh A, Taisne B (2019b) Dike Channelization and Solidification: Time Scale Controls on the Geometry and Placement of Magma Migration Pathways. J Geophys Res Solid Earth 124(9):9580-9599. https://doi.org/10.1029/2019JB018191

Perugini D, Kueppers U (2012) Fractal analysis of experimentally generated pyroclasts: a tool for volcanic hazard assessment. Acta Geophys 60(3):682-698. https://doi.org/10.2478/s11600-012-0019-7

Pioli L, Bonadonna C, Azzopardi BJ, et al (2012) Experimental constraints on the outgassing dynamics of basaltic magmas. J Geophys R: Solid Earth 117(B3). https://doi.org/10.1029/2011JB008392

Poppe S, Holohan EP, Pauwels E, et al (2015) Sinkholes, pit craters, and small calderas: Analog models of depletioninduced collapse analyzed by computed X-ray microtomography. Bull Geol Soc Am 127:281–296. https://doi.org/10.1130/B30989.1

Poppe S, Holohan EP, Galland O, et al (2019) An Inside Perspective on Magma Intrusion: Quantifying 3D Displacement and Strain in Laboratory Experiments by Dynamic X-Ray Computed Tomography. Front Earth Sci 7:62. https://doi.org/10.3389/feart.2019.00062

Poppe S, Holohan EP, Rudolf M, et al (2021) Mechanical properties of quartz sand and gypsum powder (plaster) mixtures: Implications for laboratory model analogues for the Earth’s upper crust. Tectonophysics 814:228976. https://doi.org/10.1016/J.TECTO.2021.228976

Qin Z, Soldati A, Velazquez Santana LC, et al (2018) Slug Stability in Flaring Geometries and Ramifications for Lava Lake Degassing. J Geophys Res Solid Earth 123:10,431-10,448. https://doi.org/10.1029/2018JB016113

Reber JE, Cooke ML, Dooley TP (2020) What model material to use? A Review on rock analogs for structural geology and tectonics. Earth-Science Reviews 202:103107. https://doi.org/10.1016/j.earscirev.2020.103107

Ripepe M, Rossi M, Saccorotti G (1993) Image processing of explosive activity at Stromboli. J Volcanol Geotherm

Res 54(3-4):335-51. https://doi.org/10.1016/0377-0273(93)90071-X
Rivalta E, Büttinger M, Dahm T (2005) Buoyancy-driven fracture ascent: Experiments in layered gelatine. J Volcanol Geotherm Res 144:273–285. https://doi.org/10.1016/j.jvolgeores.2004.11.030
Rivalta E, Taisne B, Bunger AP, Katz RF (2015) A review of mechanical models of dike propagation: Schools of thought, results and future directions. Tectonophysics 638:1–42. https://doi.org/10.1016/j.tecto.2014.10.003
Roche O (2012) Depositional processes and gas pore pressure in pyroclastic flows: An experimental perspective. Bull Volcanol 74:1807–1820. https://doi.org/10.1007/s00445-012-0639-4
Roche O, Carazzo G (2019) The contribution of experimental volcanology to the study of the physics of eruptive processes, and related scaling issues: A review. J Volcanol Geotherm Res 384:103–150. https://doi.org/10.1016/J.JVOLGEORES.2019.07.011
Roche O, Druitt TH, Merle O (2000) Experimental study of caldera formation. J Geophys Res 105:395. https://doi.org/10.1029/1999JB900298
Roche O, Niño Y, Mangeney A, et al (2013) Dynamic pore-pressure variations induce substrate erosion by pyroclastic flows. Geology 41:1107–1110. https://doi.org/10.1130/G34668.1
Romine WL, Whittington AG, Nabelek PI, Hofmeister AM (2012) Thermal diffusivity of rhyolitic glasses and melts: effects of temperature, crystals and dissolved water. Bull Volcanol 74(10):2273-2287. https://doi.org/10.1007/s00445-012-0661-6
Rowell CR, Jellinek M, Gilchrist J (2020) Tracking time-dependent eruption source unsteadiness and local entrainment in ground-based thermal imagery using spectral-clustering. AGU Fall Meeting Abstracts 2020:V008-0015. https://ui.adsabs.harvard.edu/abs/2020AGUFMV008.0015R
Ruch J, Acocella V, Geshi N, et al (2012) Kinematic analysis of vertical collapse on volcanoes using experimental models time series. J Geophys Res 117:B07301. https://doi.org/10.1029/2012JB009229
Rumpf ME, Lev E, Wysocki R (2018) The influence of topographic roughness on lava flow emplacement. Bull Volcanol 80:. https://doi.org/10.1007/s00445-018-1238-9
Rust AC, Cashman KV (2011) Permeability controls on expansion and size distributions of pyroclasts. J Geophys Res Solid Earth 116(B11). https://doi.org/10.1029/2011JB008494
Rust AC, Cashman KV (2004) Permeability of vesicular silicic magma: inertial and hysteresis effects. Earth Planet Scie Lett 228(1-2):93-107. https://doi.org/10.1016/j.epsl.2004.09.025
Salvatore V, Cigala V, Taddeucci J, et al (2020) Gas-Pyroclast Motions in Volcanic Conduits During Strombolian Eruptions, in Light of Shock Tube Experiments. J Geophys Res Solid Earth 125:. https://doi.org/10.1029/2019JB019182
Saxby J, Beckett F, Cashman K, et al (2018) The impact of particle shape on fall velocity: Implications for volcanic ash dispersion modelling. J Volcanol Geotherm Res 362:32-48. https://doi.org/10.1016/j.jvolgeores.2018.08.006
Schepp LL, Ahrens B, Balcewicz M, et al (2020) Digital rock physics and laboratory considerations on a high-porosity volcanic rock. 1–16. https://doi.org/10.1038/s41598-020-62741-1
Schmid M, Kueppers U, Cigala V, et al (2020) Release characteristics of overpressurised gas from complex vents: implications for volcanic hazards. Bull Volcanol 82(11):1-12. https://doi.org/10.1007/s00445-020-01407-2
Schmiedel T, Galland O, Haug T, et al (2019) Coulomb failure of Earth's brittle crust controls growth, emplacement and shapes of igneous sills, saucer-shaped sills and laccoliths. Earth Planet Sci Lett 510:161–172. https://doi.org/10.1016/j.epsl.2019.01.011
Seropian G, Stix J (2018) Monitoring and forecasting fault development at actively forming calderas: An experimental study. Geology 46:23–26. https://doi.org/10.1130/G39551.1
Seyfried R, Freundt A (2000) Experiments on conduit flow and eruption behavior of basaltic volcanic eruptions. J Geophys Res Solid Earth 105:23727–23740. https://doi.org/10.1029/2000jb900096
Sher D, Woods AW (2017) Experiments on mixing in pyroclastic density currents generated from short-lived volcanic explosions. Earth Planet Sci Lett 467:138-148. https://doi.org/10.1016/j.epsl.2017.03.009.
Smith G, Rowley P, Williams R, et al (2020) A bedform phase diagram for dense granular currents. Nat Commun 11(1):2873. https://doi.org/10.1038/s41467-020-16657-z.
Soldati A, Farrell JA, Wysocki R, Karson JA (2021) Imagining and constraining ferrovolcanic eruptions and landscapes through large-scale experiments. Nat Comm 12:1711. https://doi.org/10.1038/s41467-021-21582-w
Sonder I, Graettinger AH, Valentine GA (2015) Scaling multiblast craters: General approach and application to volcanic craters. J Geophys Res Solid Earth 120(9):6141-58. https://doi.org/10.1002/2015JB012018
Sonder I, Harp A, Graettinger AH, et al (2018). Meter-scale experiments on magma-water interaction. J Geophys Res Solid Earth 123:10,597–10,615. https://doi.org/10.1029/2018JB015682

Soule SA, Cashman K V. (2004) The mechanical properties of solidified polyethylene glycol 600, an analog for lava crust. J Volcanol Geotherm Res 129:139–153. https://doi.org/10.1016/S0377-0273(03)00237-3
Spina L, Cimarelli C, Scheu B, et al (2016) On the slow decompressive response of volatile- and crystal-bearing magmas: An analogue experimental investigation. Earth Planet Sci Lett 433:44–53. https://doi.org/10.1016/j.epsl.2015.10.029
Stevenson RJ, Bagdassarov NS, Dingwell DB, Romano C (1998) The influence of trace amounts of water on the viscosity of rhyolites. Bull Volcanol 60(2):89-97. https://doi.org/10.1007/s004450050218
Sulpizio R, Castioni D, Rodriguez-Sedano LA, et al (2016) The influence of slope-angle ratio on the dynamics of granular flows: insights from laboratory experiments. Bull Volcanol 78(11):77. https://doi:10.1007/s00445-016-1069-5.
Taddeucci J, Alatorre-Ibarguengoitia MA, Palladino DM, et al (2015) High-speed imaging of Strombolian eruptions: Gas-pyroclast dynamics in initial volcanic jets. Geophys Res Lett 42:6253–6260. https://doi.org/10.1002/2015GL064874
Taisne B, Jaupart C (2009) Dike propagation through layered rocks. J Geophys Res Solid Earth 114(B9). https://doi.org/10.1029/2008JB006228
Taisne B, Tait S (2009) Eruption versus intrusion? arrest of propagation of constant volume, buoyant, liquid-filled cracks in an elastic, brittle host. J Geophys Res Solid Earth 114:1–7. https://doi.org/10.1029/2009JB006297
Taisne B, Tait S (2011) Effect of solidification on a propagating dike. J Geophys Res Solid Earth 116:1–14. https://doi.org/10.1029/2009JB007058
Touvet T, Balmforth NJ, Craster R V, Sutherland BR (2011) Fingering instability in buoyancy-driven fluid-filled cracks. J Fluid Mech 672:60–77. https://doi.org/10.1017/S0022112010005860
Valentine GA (2020) Initiation of dilute and concentrated pyroclastic currents from collapsing mixtures and origin of their proximal deposits. Bull Volcanol 82:20. https://doi.org/10.1007/s00445-020-1366-x
Valentine GA, Graettinger AH, Macorps É, et al (2015) Experiments with vertically and laterally migrating subsurface explosions with applications to the geology of phreatomagmatic and hydrothermal explosion craters and diatremes. Bull Volcanol 77(3):1-7. https://doi.org/10.1007/s00445-015-0901-7
Van Eaton AR, Amigo Á, Bertin D, et al (2016) Volcanic lightning and plume behavior reveal evolving hazards during the April 2015 eruption of Calbuco volcano, Chile. Geophys Res Lett 43:3563– 3571. https://doi.org/10.1002/2016GL068076
Wadge G, Voight B, Sparks RSJ et al (2014) An overview of the eruption of Soufriere Hills Volcano, Montserrat from 2000 to 2010. Mem Geol Soc London 39:1–40. https:// doi. org/ 10. 1144/ M39.1
Watson LM (2020) Using unsupervised machine learning to identify changes in eruptive behavior at Mount Etna, Italy. J Volcanol Geotherm Res 405, 107042. https://doi.org/10.1016/j.jvolgeores.2020.107042
Weit A, Roche O, Dubois T, Manga M (2018) Experimental Measurement of the Solid Particle Concentration in Geophysical Turbulent Gas-Particle Mixtures. J Geophys Res Solid Earth, 123(5):3747-3761. https://doi.org/10.1029/2018JB015530
Witham F, Woods AW, Gladstone C (2006) An analogue experimental model of depth fluctuations in lava lakes. Bull Volcanol 69:51–56. https://doi.org/10.1007/s00445-006-0055-8
Zhu J, Liu X, Shi Q, et al (2020) Development trends and perspectives of future sensors and MEMS/NEMS. Micromachines 11:. https://doi.org/10.3390/mi11010007
Zorn EU, Walter TR, Heap MJ, Kueppers U (2020) Insights into lava dome and spine extrusion using analogue sandbox experiments. Earth Planet Sci Lett 551:116571. https://doi.org/10.1016/j.epsl.2020.116571

Table 1 Key parameter ranges for analog experiments versus their natural counterparts

	Parameter [Units]	Physical description	Experiments	Nature	References
Magma intrusion	h [m]	overburden height	$0.06 - 0.10$	$10^1 - 10^4$	Mathieu et al., 2008; Galland et al., 2014; Poppe et al., 2019
	B [m]	dike transverse breadth	< 0.4	$10^2 - 10^4$	Kavanagh et al. 2018a, b; Pansino et al. 2019a, b
	C [kg m^{-1} s^{-2}]	solid cohesion	$1 - 700$	$10^5 - 10^7$	Galland et al. 2006, 2014; Abdelmalak et al. 2016; Schmiedel et al. 2019; Poppe et al. 2019, 2021
	E [kg m^{-1} s^{-2}]	Young's modulus	$10^3 - 10^4$	30×10^9	Kavanagh et al. 2013; Pansino & Taisne 2019
	G [kg m^{-1} s^{-2}]	shear modulus	$10^3 - 10^4$	30×10^9	Rivalta et al. 2005
	H [m]	dike thickness	$10^{-3} - 10^{-2}$	$10^{-2} - 10$	Pansino et al. 2019a, b
	K_c [kg m$^{-0.5}$ s^{-2}]	critical fracture toughness	$40 - 170$	10^6	Meredith & Atkinson 1985; Kavanagh et al. 2013
	L [m]	dike axial length	< 0.4	$10^2 - 10^4$	Kavanagh et al. 2018a, b; Pansino et al. 2019a, b
	Q [m^3 s^{-1}]	volumetric flow rate	$10^{-8} - 10^{-5}$	$10^{-2} - 10^2$	Pansino et al. 2019a, b
	T [°C]	tempreature	$30 - 70$	$700 - 1400$	Taisne & Tait 2011; Pansino et al. 2019a, b
	T_0	solid tensile strength	$5 - 200$	$10^5 - 10^7$	Abdelmalak et al., 2016; Poppe et al., 2021
	α [m^2 s^{-1}]	thermal diffusivity	10^{-7} †	$10^{-7} - 10^{-6}$	Hartlieb et al. 2016; Pansino et al. 2019a, b
	ρ_s [kg m^{-3}]	solid crust density	$1000 - 1050$	$1600 - 3000$	Gailler et al. 2009; Kavanagh et al. 2013; Guldstrand et al. 2017
	ρ_l [kg m^{-3}]	liquid magma density	$\sim 0 - 1440$	$\sim 40 - 2700$	Rivalta et al. 2005; Galland et al. 2006; Mathieu et al. 2008; Taisne & Tait 2009; Schepp et al. 2020
	$\Delta\rho$ [kg m^{-3}]	crust-fluid density contrast	$370 - 1000$	$400 - 3000$	Rivalta et al. 2005; Taisne & Jaupart 2009
	γ [kg s^{-2}]	surface energy	1	1	Kavanagh et al. 2013
	μ [kg m^{-1} s^{-1}]	fluid dynamic viscosity	$10^{-5} - 10^{-1}$	$1 - 10^{12}$ ‡	Rivalta et al. 2005; Gonnerman 2015; Kavanagh et al. 2018a, b; Pansino & Taisne 2019
	ϕ [degrees]	solid internal friction angle	$21 - 35$	$25 - 45$	Galland et al. 2006; Galland et al. 2014; Abdelmalak et al. 2016; Schmiedel et al. 2019; Poppe et al. 2019, 2021
	ν	Poisson's ratio	0.5	0.25	Rivalta et al. 2005
	A/C	activation/cooling time ratio	0.2	$0.1 - 0.2$	Derrien and Taisne 2019
	L*	dimensionless length	< 10	$10^{-1} - 10^2$	Taisne & Tait 2009
	Re	Reynolds number	$< 10^2$	10	Lister & Kerr 1991; Touvet et al. 2011; Galland et al. 2014
	Θ	dimensionless temperature	$0.76 - 1$	$0.9 - 0.95$	Taisne & Tait 2011; Pansino et al. 2019a, b
	Φ	dimensionless thermal flux	$10^{-2} - 10$	$10^{-3} - 10^2$	Taisne & Tait 2011; Pansino et al. 2019a, b

† gelatin
‡ gas-poor/rich

Table 1: Continued

	Parameter [Units]	Physical description	Experiments	Nature	References
Gravitational deformation (chronic)	g [m s^{-2}]	gravitational acceleration	9.81	3.70 (Mercury) 8.87 (Venus) 9.81 (Earth) 3.69 (Mars)	Merle & Borgia 1996; Delcamp et al. 2008; Kervyn et al. 2010; Byrne et al. 2013
	B [m]	brittle layer thickness	$10^{-2} - 10^{-1}$	$10^{3} - 10^{5}$	Merle & Borgia 1996; Delcamp et al. 2008; Kervyn et al. 2010; Byrne et al. 2013
	D [m]	ductile layer thickness	10^{-1}	$10^{3} - 10^{5}$	Merle & Borgia 1996; Delcamp et al. 2008; Kervyn et al. 2010; Byrne et al. 2013
	E [Pa]	Young's modulus	5×10^{6}	7.5×10^{10}	Merle & Borgia 1996; Delcamp et al. 2008; Kervyn et al. 2010; Byrne et al. 2013
	H [m]	Cone height	10^{-2}	$10^{3} - 10^{5}$	Merle & Borgia 1996; Delcamp et al. 2008; Kervyn et al. 2010; Byrne et al. 2013
	P [m]	decollement thickness	10^{-4}	$1 - 10^{3}$	Byrne et al. 2013
	Q [m]	decollement depth	10^{-3}	$0 - 10^{3}$	Byrne et al. 2013
	R [m]	cone radius	$10^{-}1$	$10^{3} - 10^{5}$	Merle & Borgia 1996; Delcamp et al. 2008; Kervyn et al. 2010; Byrne et al. 2013
	S [m s^{-1}]	velocity of deformation	$10^{-6} - 10^{-5}$	$10^{-12} - 10^{-10}$	Merle & Borgia 1996; Delcamp et al. 2008; Kervyn et al. 2010; Byrne et al. 2013
	T [s]	time span of spreading	3×10^{5}	$10^{12} - 10^{13}$	Kervyn et al. 2010
	T_0 [Pa]	brittle cohesion	10^{2}	$10^{6} - 10^{8}$	Merle & Borgia 1996; Delcamp et al. 2008; Kervyn et al. 2010; Byrne et al. 2013
	μ [Pa s]	ductile material viscosity	$10^{3} - 10^{4}$	$10^{20} - 10^{22}$	Merle & Borgia 1996; Delcamp et al. 2008; Kervyn et al. 2010; Byrne et al. 2013
	ρ_b [kg m^{-3}]	brittle material density	$10^{3} - 10^{4}$	$10^{3} - 10^{5}$	Merle & Borgia 1996; Delcamp et al. 2008; Kervyn et al. 2010; Byrne et al. 2013
	ρ_d [kg m^{-3}]	ductile material density	10^{3}	$3.3 - 3.5 \times 10^{3}$	Merle & Borgia 1996; Delcamp et al. 2008; Kervyn et al. 2010; Byrne et al. 2013
	v	Poission's ratio	0.2	0.3	Merle & Borgia 1996; Delcamp et al. 2008; Kervyn et al. 2010; Byrne et al. 2013
	Θ	brittle friction coefficient	0.63	0.65	Merle & Borgia 1996; Delcamp et al. 2008; Kervyn et al. 2010; Byrne et al. 2013

Table 1: Continued

	Parameter [Units]	Physical description	Experiments	Nature	References
Caldera faulting	C_m [Pa]	brittle cohesion	$0-3\times10^2$	10^5-10^8	Holohan et al. 2008; Ruch et al. 2012; Poppe et al. 2015
	G_r [km^3 ka^{-1}]	cone growth rate	10^{-11}	$10^{-2}-10$	Grosse et al. 2020
	L [m]	length	$10^{-2}-10^{-1}$	$10^{-2}-10^4$	Roche et al. 2000; Holohan et al. 2008; Ruch et al. 2012; Poppe et al. 2015
	T_{mr} [s]	chamber residence time	10^3-10^4	$10^{12}-10^{14}$	Holohan et al. 2008
	V_{mc} [m s^{-1}]	caldera collapse velocity	$10^{-7}-10^{-6}$	$10^{-2}-10^{-1}$	Holohan et al., 2008; Ruch et al., 2012; Poppe et al., 2015
	V_{mr} [m s^{-1}]	strike-slipe velocity	$10^{-6}-10^{-4}$	$10^{-10}-10^{-8}$	Holohan et al., 2008; Grosse et al. 2020
	μ_m [Pa s]	magma viscosity	$50-10^4$	10^4-10^12	Roche et al. 2000; Holohan et al. 2008; Ruch et al. 2012; Poppe et al. 2015
	ϕ_m [°]	angle of internal friction	$22-37$	$30-45$	Roche et al. 2000; Holohan et al. 2008; Ruch et al. 2012; Poppe et al. 2015
	ρ_m [kg m^{-3}]	brittle material density	1400	$2600-3000$	Roche et al. 2000; Holohan et al. 2008; Ruch et al. 2012; Poppe et al. 2015
Domes and lava flows	C_p [J kg^{-1} K^{-1}]	heat capacity	1200	1200	Rumpf et al. 2018
	R_H [m]	resurgent dome height	10^{-2}	$1-10^3$	Brothelande et al. 2016
	R_L [m]	resurgent dome length	3×10^{-1}	10^3-10^4	Brothelande et al. 2016
	R_W [m]	resurgent dome width	10^{-1}	10^3-10^4	Brothelande et al. 2016
	T [C°]	temperature	$900-1473$	$700-1600$	Griffiths 2000; Rumpf et al. 2018 and references therein; Sonder et al. 2018; Soldati et al. 2021
	α [m^2 s^{-1}]	thermal diffusivity	$10^{-7}-10^{-6}$	$10^{-7}-10^{-6}$	Romine et al. 2012; Rumpf et al. 2018
	ρ [kg m^3]	density	$890-2700$	$900-2500$	Kavanagh et al. 2018a, b; Rumpf et al. 2018; Sonder et al. 2018
	μ [Pa s]	dynamic viscosity	$10^{-5}-10^14$	$10-10^11$	Huppert et al. 1982; Stevenson et al. 1998; Kavanagh et al. 2018a, b; Rumpf et al. 2018; Sonder et al. 2018
	Φ_g	gas volume fraction	$0.10-0.80$	$0-0.95$	Rust and Cashman 2004, 2011; Oppenheimer et al. 2015; Gonnerman 2015; Gonnerman et al. 2017; Fauria and Manga 2018
	Ψ	flow regime parameter	$2.24-2060$	$33-118$	Fink and Griffiths 1990; Gregg and Fink 2000; Rumpf et al. 2018
	Pe	Péclet number	10^4-10^5	10^2-10^8	Griffiths 2000; Rumpf et al. 2018
	Re	Reynolds number	$7.4\times10^{-3}-24$	$10^{-10}-10^6$	Huppert et al. 1984; Huppert and Sparks 1985; Griffiths 2000; Rumpf et al. 2018

Table 1: Continued

	Parameter [Units]	Physical description	Experiments	Nature	References
Cratering	d [m]	depth of explosion	$0-1$	$10-10^2$	Graettinger et al. 2014; Sonder et al. 2015
	d_p [m]	particle diameter	$0.1-5$	$10^{-2}-10^3$	Graettinger et al. 2014; Graettinger and Valentine 2017
	h [m]	jet height	$0.1-20$	$10-10^3$	Graettinger et al. 2014; Ort et al. 2018
	kg [kg]	mass of ejecta	10^2-10^3	10^2-10^8	Ripepe et al. 1993; Kilgour et al. 2010; Graettinger et al. 2014; Lube et al. 2014
	m [m]	max ballistic ejecta distance	$0.5-50$	$10-10^3$	Graettinger et al. 2014; Ort et al. 2018
	t_{pulse} [seconds]	eruption explosion interval	$10^{-3}-10^4$	$> 10^{-1}$	Dürig et al. 2015; Graettinger et al. 2018; Neilsen et al. 2019; Gilchrist et al. 2020; Rowell et al. 2020
	d_c [m]	crater depth	(-0.1)–(-0.5)	$10-10^2$	Sonder et al. 2015; Graettinger 2018
	D_{sc} [m J$^{-1/3}$]	scaled depth	$10^{-3}-10^{-2}$	$10^{-3}-10^{-2}$	Sonder et al. 2015; Valentine et al. 2015
	E [J]	explosion energy	10^5-10^7	10^9-10^15	Graettinger et al. 2014; Sonder et al. 2015
	W_c [m]	crater diameter	$0.3-6$	$10-10^3$	Graettinger et al. 2014; Sonder et al. 2015
Volcanic jets and plumes	d_p [m]	particle diameter	$10^{-5}-10^{-3}$	$10^{-6}-10^{-2}$	Dellino et al. 2010; Carazzo & Jellinek 2012
	f_{ftn} [s^{-1}]	fountain frequency	$10^{-2}-10^{-1}$	$10^{-4}-1$	Gilchrist & Jellinek 2021
	r_0 [m]	source radius	$10^{-3}-1$	$10-10^2$	Dellino et al. 2010; Carazzo & Jellinek 2012
	t_{pulse} [seconds]	eruption explosion interval	$10^{-2}-10^2$	$> 10^{-1}$	Dürig et al. 2015; Gilchrist et al. 2020; Rowell et al. 2020
	u_0 [m/s]	source speed	$10^{-3}-10^3$	$10-10^3$	Kieffer and Sturtevant 1984; Dellino et al. 2010; Carazzo & Jellinek 2012; Gilchrist & Jellinek 2021
	u_p [m/s]	particle settling speed	$0.1-1$	$10^{-1}-10^2$	Carazzo & Jellinek 2012; Saxby et al. 2018; Gilchrist & Jellinek 2021
	H_{ftn} [m]	fountain/jet height	0.1	10^3-10^4	Gilchrist & Jellinek 2021
	H_{pl} [m]	plume height	0.1	10^3-10^4	Gilchrist & Jellinek 2021
	H_{OS} [m]	overshoot height	$10^{-2}-10^{-1}$	10^3-10^4	Gilchrist & Jellinek 2021
	N [s^{-1}]	buoyancy frequency	10^{-1}	10^{-2}	Carazzo & Jellinek 2012
	μ [kg m^{-1} s^{-1}]	fluid dynamic viscosity	10^{-3}	10^{-5}	Carazzo & Jellinek 2012
	ρ_a [kg m^{-3}]	ambient fluid density	$998-1040$	$10^{-3}-1$	Carazzo & Jellinek 2012; Gilchrist and Jellinek 2021
	ρ_f [kg m^{-3}]	interstitial fluid density	$998-1050$	$0.1-1$	Carazzo & Jellinek 2012; Gilchrist and Jellinek 2021
	ρ_s [kg m^{-3}]	solid (particle) density	$42-3210$	$750-2500$	Carey et al. 1988; Carazzo & Jellinek 2012; Carazzo et al. 2015; Gilchrist and Jellinek 2021
	ϕ_0	particle volume fraction	$10^{-3}-10^{-2}$	$10^{-4}-10^{-1}$	Carazzo & Jellinek 2012; Jessop et al. 2016; Gilchrist & Jellinek 2021
	e	restitution coefficient	$0-0.85$	$0-0.85$	Cagnoli and Manga 2003; Dufek et al. 2009
	Ma	source Mach number	< 3.8	< 1.7	Kieffer and Sturtevant 1984; Orescanin et al. 2014; Schmid et al. 2020

Table 1: Continued

	Parameter [Units]	Physical description	Experiments	Nature	References
	Re_0	source Reynolds number	$3000 - 12000$	$10^7 - 10^9$	Carazzo & Jellinek 2012
	Re_p	particle Reynolds number	$1.3 - 6.5$	$10^{-4} - 10^6$	Carazzo & Jellinek 2012; Gilchrist and Jellinek 2021
	Ri_0	source Richardson number	$10^{-7} - 1$	$10^{-3} - 10$	Carazzo & Jellinek 2012; Carazzo et al. 2014; Carazzo et al. 2015; Jessop et al. 2016; Gilchrist and Jellinek 2021
	St_0	source Stokes number	$0.2 - 6.0$	$10^{-2} - 10^2$	Carazzo & Jellinek 2012; Jessop et al. 2016; Gilchrist & Jellinek 2021
	Σ_0	source stability number	$10^{-3} - 10^{-2}$	$10^{-3} - 1$	Carazzo & Jellinek 2012; Jessop et al. 2016; Gilchrist & Jellinek 2021
Pyroclastic density currents	d_p [m]	particle diameter	$10^{-6} - 10^{-2}$	$10^{-6} - 1$	Dellino et al. 2007; Andrews & Manga, 2012; Roche, 2012; Lube et al. 2015; Brosch & Lube 2019
	u [m s^{-1}]	bulk speed	$0.1 - 10$	$5 - 200$	Dellino et al. 2007; Andrews & Manga, 2012; Roche, 2012; Lube et al. 2015; Brosch & Lube 2019
	H [m]	flow height	$0.01 - 5$	$10 - 1000$	Dellino et al. 2007; Andrews & Manga, 2012; Roche, 2012; Lube et al. 2015; Brosch & Lube 2019
	KE [J m^{-3}]	kinetic energy density	10^{-2}-10^3	10^{-2}-10^4	Dellino et al. 2007; Andrews & Manga, 2012; Roche, 2012; Lube et al. 2015; Brosch & Lube 2019
	TEb [J m^{-3}]	buoyant thermal energy	10^1-10^3	10^3-10^4	Dellino et al. 2007; Andrews & Manga, 2012; Roche, 2012; Lube et al. 2015; Brosch & Lube 2019
	μ [kg m^{-1} s^{-1}]	interstitial fluid dynamic viscosity	$1.8\text{-}4 \times 10^{-5}$	$1.8\text{-}3.5 \times 10^{-5}$	Dellino et al. 2007; Andrews & Manga, 2012; Roche, 2012; Lube et al. 2015; Brosch & Lube 2019
	μ_{pp}	internal friction coefficient	$26 - 40$	$35 - 40$	Roche et al. 2012; Lube et al. 2015
	μ_b [degrees]	basal friction coefficient	$35 - 40$	$35 - 40$	Lube et al. 2015
	ρ_a [kg m^{-3}]	ambient fluid density	$1.2 - 1.3$	$1.1 - 1.3$	Dellino et al. 2007; Andrews & Manga, 2012; Roche, 2012; Lube et al. 2015; Brosch & Lube 2019
	ρ_f [kg m^{-3}]	interstitial fluid density	$0.6 - 1.2$	$0.6 - 1.2$	Dellino et al. 2007; Andrews & Manga, 2012; Roche, 2012; Lube et al. 2015; Brosch & Lube 2019
	ρ_s [kg m^{-3}]	solid density	$350 - 2900$	$350 - 2900$	Dellino et al. 2007; Andrews & Manga, 2012; Roche, 2012; Lube et al. 2015; Brosch & Lube 2019
	e	restitution coefficient	$0 - 0.85$	$0 - 0.85$	Cagnoli and Manga 2003; Dufek et al. 2009
	C	source particle concentration	$10^{-5} - 0.7$	$10^{-5} - 0.7$	Andrews and Manga, 2012; Lube et al. 2015;
	Fr	densimetric Froude number	$0.5 - 5$	$0.5 - 5$	Dellino et al. 2007; Andrews & Manga, 2012; Roche, 2012; Lube et al. 2015; Brosch & Lube 2019
	I	inertial number	$10^{-6} - 10$	$10^{-6} - 10$	Breard et al. 2020
	N	pore pressure	$0- > 1$	$0- > 1$	Druitt et al. 2007; Roche 2012; Breard et al. 2019

Table 1: Continued

	Parameter [Units]	Physical description	Experiments	Nature	References
	Re	Reynolds number	10^1-10^3	10^6-10^{10}	Dellino et al. 2007; Andrews & Manga, 2012; Roche, 2012; Lube et al. 2015; Brosch & Lube 2019
	Ri	Richardson number	0.01 – 10	0 – 10	Dellino et al. 2007; Andrews & Manga, 2012; Roche, 2012; Lube et al. 2015; Brosch & Lube 2019
	$\mathrm{Ri_t}$	thermal Richardson number	0.02 – 4.5	0 – 5	Dellino et al. 2007; Andrews & Manga, 2012; Roche, 2012; Lube et al. 2015; Brosch & Lube 2019
	Pn	Rouse number	0.7 – 10	10^{-3}-10^{-1}	Dellino et al. 2007; Andrews & Manga, 2012; Roche, 2012; Lube et al. 2015; Brosch & Lube 2019
	Ψ	grain sphericity	0.4 – 1	0.4 – 1	Dellino et al. 2005
	Σ	stability number	10^{-2}-10	10^{-6}-10^5	Dellino et al. 2007; Andrews & Manga, 2012; Roche, 2012; Lube et al. 2015; Brosch & Lube 2019
	St	Stokes number	10^{-6}-10	10^{-6}-10	Dellino et al. 2007; Andrews & Manga, 2012; Roche, 2012; Lube et al. 2015; Brosch & Lube 2019
	Str	Strouhal number	0.3	0.3	Dellino et al. 2007; Andrews & Manga, 2012; Roche, 2012; Lube et al. 2015; Brosch & Lube 2019
Debris flows	d_p [m]	particle diameter	$10^{-6} - 10^{-1}$	$10^{-6} - 1$	Iverson et al. 2010; Iverson 2012
	k [m^2]	hydraulic permeability	$10^{-12} - 5 \times 10^{-10}$	$10^{-13} - 10^{-10}$	Iverson et al. 2010; Iverson 2012
	u [m s^{-1}]	bulk speed	$1 - 10$	$1 - 50$	Iverson et al. 2010; Iverson 2012
	D [m^2]	hydraulic diffusivity	$1 - 5 \times 10^{-2}$	10^{-2}	Iverson et al. 2010; Iverson 2012
	H [m]	flow height	0.1 – 1	0.1 – 100	Iverson et al. 2010; Iverson 2012
	ρ_s [kg m^{-3}]	solid density	2000 – 2500	350 – 2900	Iverson et al. 2010; Iverson 2012
	ρ_f [kg m^{-3}]	interstitial fluid density	2000 – 2500	350 – 2900	Iverson et al. 2010; Iverson 2012
	μ [kg m^{-1} s^{-1}]	interstitial fluid dynamic viscosity	$10^{-3} - 10^{-1}$	$10^{-3} - 10^{-1}$	Iverson et al. 2010; Iverson 2012
	μ_b [degrees]	basal friction coefficient	39 – 40	~ 40	Iverson et al. 2010; Iverson 2012
	μ_{pp} [degrees]	internal friction coefficient	~ 39	~ 40	Iverson et al. 2010; Iverson 2012
	$\mathrm{N_p}$	pore pressure number	$10^{-4} - 10^{-3}$	$10^{-8} - 10^{-6}$	Iverson et al. 2010; Iverson 2012